

See discussions, stats, and author profiles for this publication at: <https://www.researchgate.net/publication/231696110>

Quantitative Analysis Method for Three-Dimensional Orientation of PTT by Polarized FTIR-ATR Spectroscopy

ARTICLE *in* MACROMOLECULES · JULY 2004

Impact Factor: 5.8 · DOI: 10.1021/ma0353033

CITATIONS

20

READS

34

3 AUTHORS, INCLUDING:



Yongri Liang

Beijing Institute of Petrochemical Technology

46 PUBLICATIONS 408 CITATIONS

SEE PROFILE



Han Sup Lee

Inha University

33 PUBLICATIONS 533 CITATIONS

SEE PROFILE

Quantitative Analysis Method for Three-Dimensional Orientation of PTT by Polarized FTIR-ATR Spectroscopy

Su Cheol Park, Yongri Liang, and Han Sup Lee*

Department of Textile Engineering, INHA University, 253 Younghyun-dong, Incheon, 402-751 Korea

Received September 4, 2003; Revised Manuscript Received May 25, 2004

ABSTRACT: Quantitative analysis method for the calculation of three-dimensional (3D) orientation of poly(trimethylene terephthalate) (PTT) with polarized FTIR-ATR spectroscopy has been discussed. To experimentally obtain a set of four ATR infrared spectra required for 3D orientation analysis, it is necessary to rotate a sample and/or polarizer by 90° upon completion of each measurement of ATR spectrum. Quality of optical contact was demonstrated to be a function of clamping pressure along two beam paths in double-edged parallelogram ATR crystal used in this work. For uniaxially stretched PTT, the band at 1410 cm⁻¹ was found to be a reference band, the absorbance of which is not affected by orientation state as well as conformation and crystallinity change. By controlling the temperature of sample and ATR crystal, the quality of optical contact could be continuously varied. It was found that the absorbance ratio of two waves (A_{TM}/A_{TE}) experimentally measured was smaller than the theoretical one unless the sample was in a completely molten state. By multiplying the normalized TM absorbance with the theoretical effective thickness ratio ($d_{e, TM}/d_{e, TE}$), three attenuation indices along three orthogonal directions were successfully obtained for uniaxially stretched PTT samples.

Introduction

FTIR-ATR spectroscopy utilizes the total internal reflection of the propagating infrared radiation occurring at the interface between the optically denser medium (ATR crystal) and optically rarer medium (sample), when the angle of incidence exceeds the critical angle. Upon reflection at the interface, the evanescent wave, the field strength of which is decaying exponentially inside the optically rare medium, might be absorbed selectively by the sample. Since the resultant reflectance infrared spectrum can be used to analyze the surface structure of the sample, ATR-FTIR spectroscopy^{1–20} is widely used for the characterization of polymeric thick films, fibers, fabrics, and coatings for which the transmission infrared method may not be easily applied.

A number of methods have been used to study the orientation status, since the physical properties of polymeric materials may be significantly affected by the orientation of polymeric chains, crystals, and domains. Infrared spectroscopy has been widely used for polymer orientation analysis since it provides the orientation information on multiple segments constituting the long polymer chain selectively. The transmission infrared method using normal incidence can provide orientation information only in two dimensions. Even though it is possible to obtain 3D orientation information with the transmission infrared method using a tilting procedure,^{21–24} it cannot be used for a thick sample for which FTIR-ATR method can be easily applied. Furthermore, FTIR-ATR can be a very useful method for quantitative 3D orientation analysis when temperature of the sample is to be controlled precisely.

Even though the FTIR-ATR method can provide unique orientation information in three orthogonal directions, it has not been extensively used for the quantitative analysis of polymer orientation due to the

inherent experimental difficulties (ED) such as ^{ED}(1) irreproducibility of optical contact between sample and ATR crystal and ^{ED}(2) dependence of the effective thickness ratio for TE and TM waves (A_{TM}/A_{TE}) on irreproducible optical contact.

To obtain three-dimensional orientation information with FTIR-ATR using a procedure initially suggested by Flournoy and Schaffers,^{1,2} a set of four different infrared spectra have to be obtained using four different experimental geometries of oriented sample and polarizer, which can be satisfied by rotating the sample and polarizer by 90°. ^{4–8,15,16} For rotation of oriented sample, the sample has to be detached from and remounted to the ATR crystal, which is the main reason for the nonuniform optical contact between sample and ATR crystal (^{ED}(1)). Three experimental methods have been introduced to solve the ^{ED}(1). The first method is to normalize all absorbance with the absorbance of the “reference band”, the absorbance of which is not affected by orientation state of sample being studied.^{11,13} Applicability of this method is limited for some polymer samples containing such a reference band. The second method to circumvent the ^{ED}(1) is to use a specially designed ATR crystal and its holder with which the rotation of oriented sample can be carried out without breaking the optical contact between sample and ATR crystal.^{5,6} The typical geometry of such a crystal is a symmetrical double-edge parallelogram of which four sides are cut to 45°, allowing two perpendicular beam paths in an ATR crystal. Even though this method has alleviated the ^{ED}(1) to some extent by maintaining the optical contact during rotation of sample, it was found that two beam paths inside an ATR crystal do not give identical optical contact mainly due to the anisotropic surface structure of the oriented sample.⁸ The last method was to use the absorbance ratio of a parallel band to a perpendicular band for the polymer chain showing cylindrical symmetry.⁸ This method, however, has been applied only to the polypropylene sample thus far.

* To whom all correspondence should be addressed. E-mail: hslee@inha.ac.kr.

Infrared dichroism of a certain band using the ATR method can be calculated by dividing two corresponding normalized absorbances of infrared spectra obtained at two specific sample positions while maintaining polarizer direction. However, spatial orientation along three directions can be calculated from four spectra obtained at two sample and polarizer directions with Flournoy and Schaffers' method. The optical contact problem occurring when rotating a sample has been discussed in the previous paragraphs. Electric field intensity of totally reflecting radiation at the interface between ATR crystal and sample depends on the polarizer direction (TE or TM mode), resulting in very different effective thickness (d_e). Furthermore, the magnitude of effective thickness at a certain polarizer direction ($d_e(\text{TE})$ or $d_e(\text{TM})$) is affected by many experimental factors such as refractive indices of sample and crystal, wavelength of infrared radiation for a specific band, and angle of incidence.³ To get the quantitatively correct result on the three-dimensional orientation using Flournoy and Schaffers' method, the effective thickness ratio ($d_e(\text{TM})/d_e(\text{TE})$) experimentally obtained has to be identical with the theoretical one.³ However, the effective thickness ratio obtained experimentally is sensitively affected by the optical contact between sample and ATR crystal. When the optical contact is not "ideal", the experimental effective thickness ratio has been reported to be smaller than the theoretical one.^{9,10} In a method suggested by Sung and co-workers, a different angle of incidence was used for two polarizer directions to ensure a desired effective thickness at two directions.⁶ In a work on the spatial orientation analysis of PET, the absorbance of a specific band was normalized with the absorbance of the 1410 cm^{-1} band that had been successfully used as a reference band in many previous works.¹³

In this work, those experimental problems mentioned above will be considered, and a method will be suggested to obtain quantitative three-dimensional orientation information using the FTIR-ATR method. Applicability of the suggested method will be tested with poly(trimethylene terephthalate) (PTT), an aromatic polyester which is extensively being studied for new candidate material for fiber and film.^{25–28}

Experimental Section

Material. PTT used in this work was synthesized with 1,3-propanediol and terephthalic acid. The intrinsic viscosity of PTT measured in dichloroacetic acid at $30\text{ }^\circ\text{C}$ was 0.84 dL/g . The synthesized PTT polymer was heated to $245\text{ }^\circ\text{C}$ for melt pressing ($T_m = 225\text{ }^\circ\text{C}$) followed by quenching into ice water to form the melt-quenched amorphous PTT film. The amorphous film was then uniaxially deformed with $10\%/s$ speed at $55\text{ }^\circ\text{C}$ ($T_g = 45\text{ }^\circ\text{C}$) inside a temperature-controlled stretcher.

ATR Measurement. For the ATR measurement, a double-edged parallelogram ATR crystal (45° cut, KRS-5, Harrick Sci. Corp.) initially designed by Sung and co-workers was used along with the rotatable sample holder.⁶ Using variable angle ATR attachment (Nicolet Corp.), the angle of incidence (θ) of the infrared radiation at the interface between ATR crystal and polymer film was set to 45° . When mounting polymer film to ATR crystal, a torque wrench was used to maintain constant pressure between them. All ATR spectra were obtained using Nicolet 520 FTIR spectrometer equipped with liquid nitrogen cooled MCT detector at 2.0 cm^{-1} resolution and 32 scans. Polarization of infrared radiation was achieved by inserting wire-grid polarizer (KRS-5, Harrick Sci. Corp.) between ATR setup and detector.

Figure 1 shows the schematic picture for the temperature-controlled ATR setup. Temperature of the sample was controlled by lab-built heating plate. A thin ceramic plate (mica)

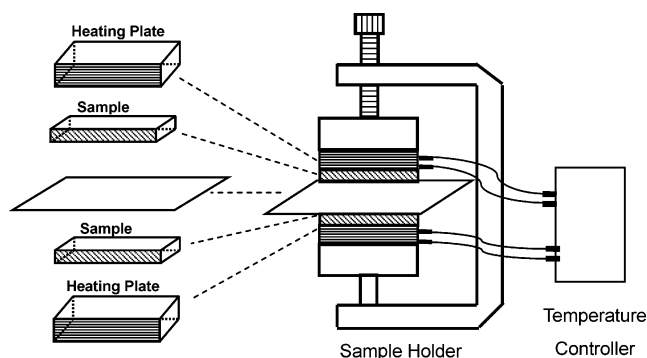


Figure 1. Temperature-controlled FTIR-ATR setup containing double-edged parallelogram ATR crystal and heating plates.

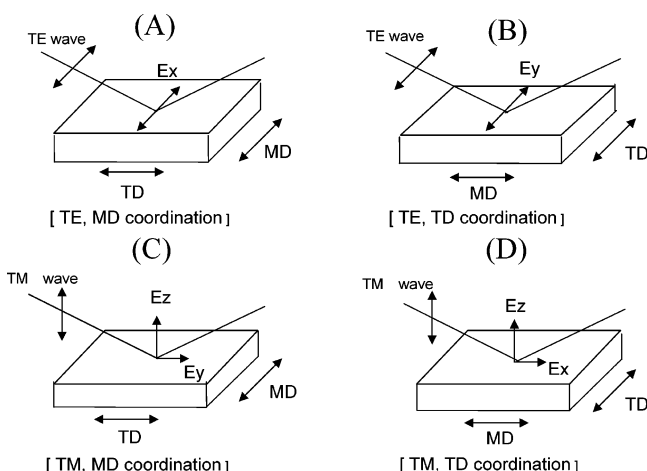


Figure 2. Coordinate systems of ATR measurements for three-dimensional orientation analysis. Polarizer direction determines either transverse electric (TE) or transverse magnetic (TM) component of incident IR radiation. The sample was stretched along the machine direction (MD(x)) for uniaxial deformation.

was wound with Nichrome wire, and the whole thing was sandwiched between two mica plates to ensure a flat surface. Three mica plates were glued together with ceramic paste.

Upon heating the sample to a certain temperature, it was maintained at that temperature at least for 3 min to ensure an equilibrium structure at that temperature before four different infrared spectra were being taken at different ATR setup (with sample) and polarizer directions. With one-dimensional ATR crystal containing only one beam path, the sample has to be detached from and remounted to the ATR crystal to obtain three-dimensional orientation information. It would be, then, impossible to maintain a constant temperature during measurements of four infrared spectra. Therefore, two-dimensional ATR crystal seems to be inevitable for the three-dimensional orientation experiment, when sample temperature has to be controlled precisely. With the ATR crystal setup used in this work, the sample inside the ATR setup could be rotated while maintaining the temperature of the sample and clamping pressure between sample and ATR crystal constant.

Results and Discussion

Figure 2 shows experimental geometries for sample and polarization directions, which are used for the measurement of four different infrared spectra required for the calculation of three-dimensional orientation information. Polarization modes (TE or TM) of the incident radiation were selected by rotating the polarizer. Sample position in the four coordinates in Figure 2 was denoted as the sample direction that is perpen-

pendicular to the plane of incidence. $A_{TM,TD}$ is, for example, absorbance of a certain band obtained with TM polarization and sample position of which TD direction is perpendicular to the plane of incidence. The three electric field components, i.e., E_x , E_y , E_z , of the incidence radiation were parallel to three principal directions, i.e., MD, TD, and ND directions of the uniaxially deformed samples, respectively. Whereas the electric component of the TE mode exists only along the film plane (Figure 2A,B), that of the TM mode consists of two components, i.e., parallel and perpendicular to the film plane. (Figure 2C,D). Three spatial attenuation indices (k_x , k_y , k_z) can be calculated using eq 1 and four absorbances ($A_{TE,MD}$, $A_{TM,MD}$, $A_{TE,TD}$, $A_{TM,TD}$) measured from a specific infrared band of four different infrared spectra obtained with four geometries in Figure 2,

$$\begin{aligned} A_{TE,MD} &= \alpha k_x \\ A_{TM,MD} &= \beta k_y + \gamma k_z \\ A_{TE,TD} &= \alpha k_y \\ A_{TM,TD} &= \beta k_x + \gamma k_z \end{aligned} \quad (1)$$

where α , β , and γ are constants, determined by the refractive indices of crystal and polymer, and angle of incidence (θ) as shown in eq 2.

$$\begin{aligned} \alpha &= \frac{4n^2 \cos \theta}{(\sin^2 \theta - n^2)^{1/2}(1 - n^2)} \\ \beta &= \frac{4n^2 \cos \theta (\sin^2 \theta - n^2)}{(\sin^2 \theta - n^2)^{1/2}(\sin^2 \theta - n^2 + n^4 \cos^2 \theta)} \\ \gamma &= \frac{4n^2 \cos \theta \sin^2 \theta}{(\sin^2 \theta - n^2)^{1/2}(\sin^2 \theta - n^2 + n^4 \cos^2 \theta)} \\ n &= \frac{\bar{n}_{\text{polymer}}}{n_{\text{crystal}}} \end{aligned} \quad (2)$$

In eqs 1 and 2, the average refractive index of polymer is used $((n_x + n_y + n_z)/3 = \bar{n}_{\text{polymer}})$. As noted from eq 2, the three constants (α , β , γ) are functions of the refractive index. If refractive indices along three directions become very different from each other upon deformation, and if dispersion effect becomes significant, three-dimensional information calculated with eq 2, then, contains a certain amount of calculation error.^{1,10} In most FTIR-ATR works on 3D orientation analysis previously published, the refractive index (n) in eq 2 is usually calculated on the basis of the refractive index of isotropic sample (\bar{n}). Provided that quantitative analysis is limited to infrared bands of low absorbance of which refractive indices are not very different from the average value, the dispersion effect could be minimized, and the calculation error was small enough not to change the general trend of calculated results.^{6,10,13,15}

As mentioned previously, optical contact between ATR crystal and sample plays an important role for accurate calculation of the three-dimensional orientation. To obtain the quantitative 3D orientation information by applying experimental FTIR-ATR spectra directly to eq 1, the optical contact has to be ideal. For most experimental conditions, it is very difficult to maintain the ideal optical contact. In the following sections, therefore, we are going to discuss various experimental problems related to the optical contact between sample and ATR

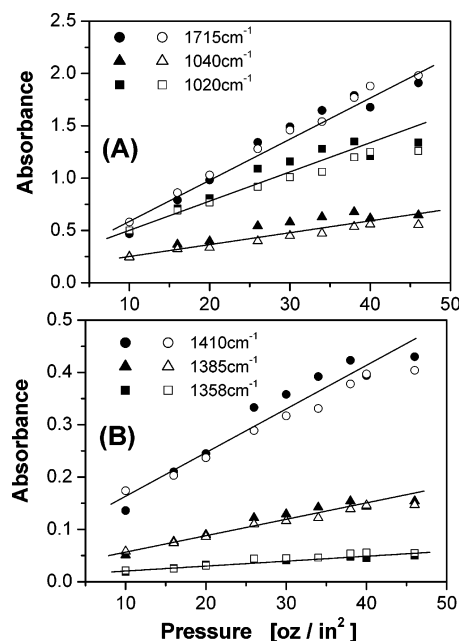


Figure 3. Absorbance change as a function of the pressure between ATR crystal and the melt-quenched amorphous PTT film. The filled and open symbols represent the absorbances obtained along two beam paths of a double-edged ATR crystal (solid, path 1; open, path 2).

crystal and its change upon rotation of sample and polarizer. The effect of optical contact change on the effective thickness of TE and TM waves will be also evaluated. As a conclusion, a new method to solve the optical contact problem will be suggested, and its applicability will be tested with uniaxially stretched PTT films.

Effect of Optical Contact between Sample and ATR Crystal on Infrared Absorbance. It was mentioned that with one-dimensional ATR crystal the sample has to be detached from and remounted to the ATR crystal in order to get 3D orientation information. To estimate the magnitude of optical contact effect on the infrared absorbance, absorbances of six infrared bands were measured as a function of clamping pressure using the melt-quenched amorphous PTT film at room temperature, and the results are shown in Figure 3. Since there is additional beam path (path 2) in two-dimensional ATR crystal, similar measurement was repeated and shown again in the same figure with open data points. It is clear that absorbance increases almost linearly with clamping pressure. Furthermore, there is some discrepancy between two corresponding absorbances obtained along two different beam paths, even though the difference may be small for some bands. These two facts appear to indicate that it will be very difficult to maintain identical optical contact if reclamping process is required as with one-dimensional ATR crystal.

The double-edged crystal used in this work was, initially, expected to solve the optical contact problem related to the reclamping process. With this ATR crystal, the spectra in four different geometries shown in Figure 2 can be obtained without breaking an optical contact between sample and ATR crystal. If we can obtain identical optical contact during measurement of a set of four different spectra, then, the normalization process with a reference band is not required. In the work reported later by Mirabella, it was found that two

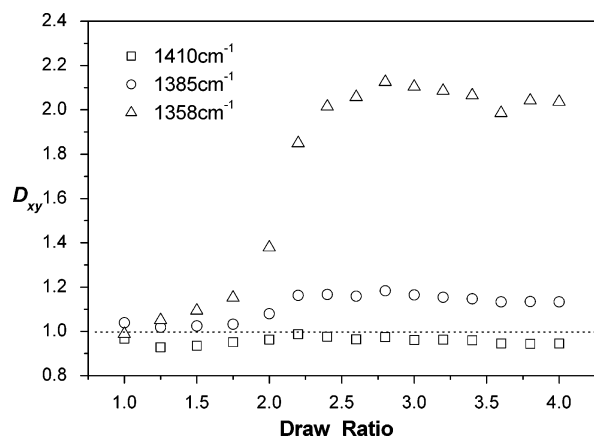


Figure 4. Dichroic ratio (D_{xy}) as a function of draw ratio.

beam paths in a double-edged parallelogram ATR crystal also do not ensure identical optical contact, especially if an anisotropic sample is used.⁸ The anisotropic surface texture was known to cause difference in the optical contact. Therefore, it can be, again, concluded that the normalization process is required even for two-dimensional ATR crystal with which a set of four spectra can be measured without breaking an optical contact.

In a paper on orientation work of uniaxially stretched PET using FTIR-ATR spectroscopy by Walls, several infrared bands were examined to be used as a reference band of which absorbance is not affected by the structural parameters such as chain orientation, conformation, and crystallinity.¹¹ By examining bands at 790, 1410, and 1510 cm^{-1} , he found out that whereas A_{TE}/A_{TM} values of 790 and 1510 cm^{-1} bands showed parallel dichroism, that of the 1410 cm^{-1} band showed practically no dichroism for all samples drawn to various draw ratios. On the basis of these results and others in subsequent works, it was confirmed that band at 1410 cm^{-1} can be used as a reference band for 3D orientation work of uniaxially stretched PET using FTIR-ATR spectroscopy.^{12,13}

Since PTT is also an aromatic polyester having a similar chemical structure as PET, we tested the applicability of 1410 cm^{-1} band as a reference band using three independent experiments. First, to evaluate the dichroic characteristics, the melt-quenched amorphous PTT films were drawn to various draw ratios inside a temperature-controlled mechanical stretcher. Using polarized infrared spectroscopy based on transmission method, dichroic ratios (D_{xy}) of three different bands were obtained, and the results are shown in Figure 4. The band at 1410 cm^{-1} is associated with the aromatic ring vibration and those at 1385 and 1358 cm^{-1} with the CH_2 wagging in amorphous and crystalline phases, respectively.²⁹ As can be seen from Figure 4, the band at 1410 cm^{-1} shows almost a constant dichroic ratio for all draw ratios, whereas those two wagging bands show parallel dichroism. This result indicates that the band at 1410 cm^{-1} does not show dichroism in the film plane (xy plane). We also measured three refractive indices along three principal directions (n_x , n_y , n_z) of uniaxially stretched PTT samples, and the results are shown in Figure 5. Before drawing, all three indices showed identical values indicative of isotropic state. Upon uniaxial drawing, n_x increases continuously, whereas n_y and n_z decrease. Furthermore, n_y values are very close to the corresponding n_z values for all draw ratios studied. These results indicate that the uniaxially

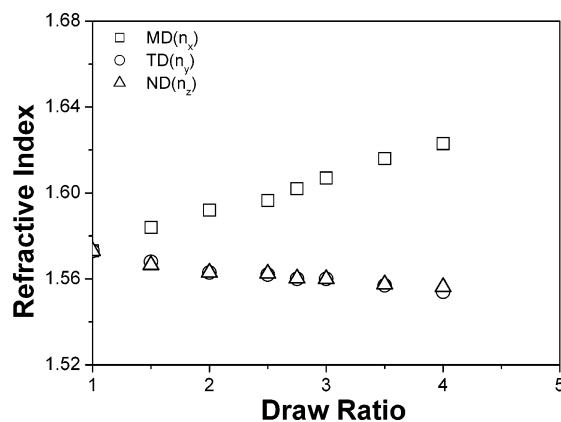


Figure 5. Three refractive indices (n_x , n_y , n_z) along MD, TD, ND directions of uniaxially stretched PTT films. Drawing rate was 10%/s at 55 $^{\circ}\text{C}$.

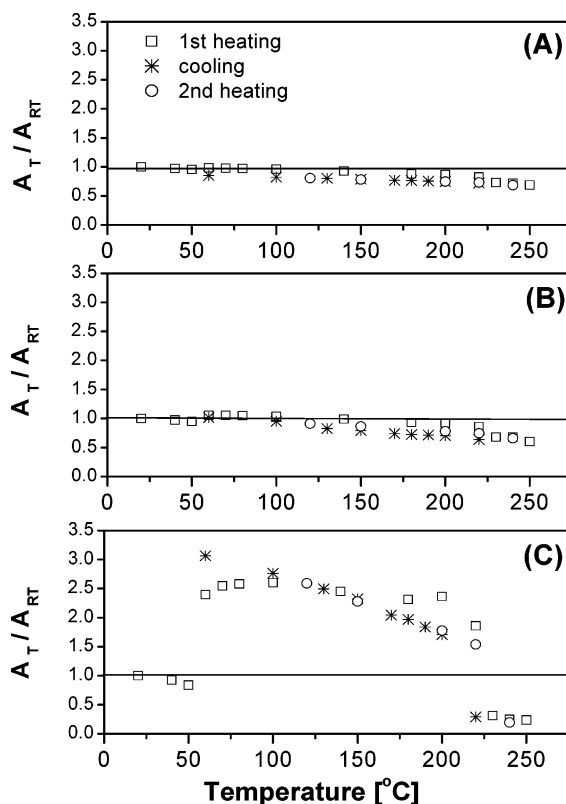


Figure 6. Relative absorbance as a function of temperature during first heating, cooling, and second heating: (A) 1410, (B) 1385, and (C) 1358 cm^{-1} .

stretched PTT sample maintains cylindrical symmetry around the deformation direction. Combining the results in Figures 4 and 5, we can conclude that the band at 1410 cm^{-1} of uniaxially stretched PTT does not show dichroism not only in the xy plane but also in the yz plane.

The last method we used to confirm the validity of the 1410 cm^{-1} band as a reference band was to examine the correlation of band absorbance with the internal structures such as conformation and crystallinity of PTT. By placing a thin amorphous PTT film between two KBr disks that are inserted into a heating block, the absorbance of three bands was measured while temperature of the sample was changed, and the results are plotted in Figure 6. Absorbance was measured during first heating, cooling, and second heating periods. For clarity, all absorbance was normalized with that at

room temperature before initial heating. From Figure 6c, it can be seen that the absorbance of the 1358 cm^{-1} band increases abruptly at about $50\text{ }^{\circ}\text{C}$, at which temperature the amorphous PTT sample used here undergoes the cold crystallization process. Upon crystallization, crystalline content increases abruptly, resulting in a sudden increase of the 1358 cm^{-1} band absorbance. As the temperature increases further up to about $220\text{ }^{\circ}\text{C}$, absorbance shows a slight increase. Upon further heating above $225\text{ }^{\circ}\text{C}$, absorbance decreases abruptly due to melting transition of PTT. If the molten PTT is slowly cooled again (data shown in stars), crystallization occurs again at about $220\text{ }^{\circ}\text{C}$, resulting in the sudden increase. Further decrease of the temperature causes gradual increase of crystalline contents. As shown in Figure 6A, the absorbance of the 1410 cm^{-1} band is not sensitively affected by the thermally induced phase changes. The fact that the 1410 cm^{-1} band does not show any abrupt intensity change upon cold crystallization ($\sim 50\text{ }^{\circ}\text{C}$), melting ($\sim 220\text{ }^{\circ}\text{C}$), and recrystallization during heating and cooling process indicates that the absorbance of the 1410 cm^{-1} band is not directly related to the chain conformation and overall crystallinity.

On the basis of the results of three independent experiments mentioned above, it could be concluded that the band at 1410 cm^{-1} can be used as a reference band for three-dimensional orientation analysis of uniaxially stretched PTT using polarized FTIR-ATR spectroscopy.

Difference in the Effective Thickness of TE and TM Waves. Absorbance of a specific band obtained from the FTIR-ATR spectrum is affected not only by those factors (orientation and quality of optical contact between sample and ATR crystal) explained in the previous section but also by polarization direction of incident IR radiation. The effective thickness for TE and TM waves ($d_{e,TE}$, $d_{e,TM}$) can be calculated with the following equations:

$$\frac{d_e(\text{TE})}{\lambda_1} = \frac{n \cos \theta}{\pi(1 - n^2)(\sin^2 \theta - n^2)^{1/2}}$$

$$\frac{d_e(\text{TM})}{\lambda_1} = \frac{n \cos \theta(2 \sin^2 \theta - n^2)}{\pi(1 - n^2)[(1 + n^2) \sin^2 \theta - n^2](\sin^2 \theta - n^2)^{1/2}}$$

$$\lambda_1 = \lambda/n_{\text{crystal}} \quad (3)$$

As can be seen from eq 3, the effective thickness of both waves is a function of refractive index of sample, angle of incidence and the wavelength of the infrared radiation. Furthermore, the effective thickness of the TM wave ($d_{e,TM}$) is always greater than that of the TE wave ($d_{e,TE}$). To analyze 3D orientation quantitatively with FTIR-ATR, therefore, it is important to consider the dependency of absorbance on the polarization direction.

When the angle of incidence is 45° , the effective thickness ratio ($d_{e,TM}/d_{e,TE}$) of two waves is 2 for any isotropic samples, which can be confirmed easily with eq 3. This means that the ratio of two absorbances (A_{TM}/A_{TE}) in eq 2 should become 2, provided that the contact between sample and ATR crystal is perfect. In many works reported already, the absorbance ratio (A_{TM}/A_{TE}) measured experimentally was about 1.3–1.7, which is well below the theoretical one.^{9,10,18} Gupta explained that deviation of experimental observation from theoretical prediction is mainly due to the false radiation

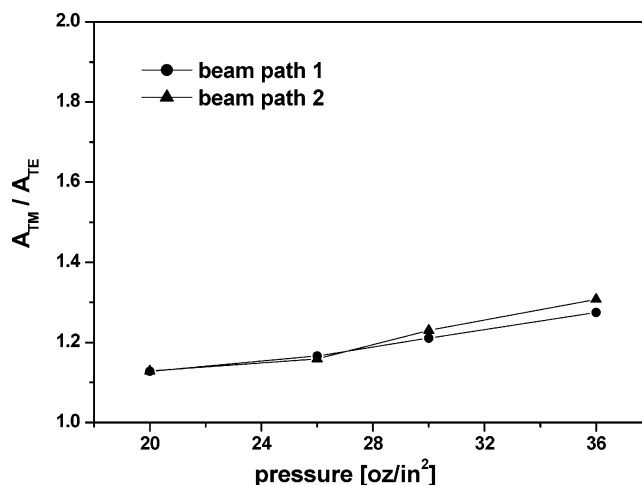


Figure 7. Absorbance ratio of TE and TM waves for the 1410 cm^{-1} band obtained along two beam paths of double-edged ATR crystal as a function of the pressure between ATR crystal and the melt-quenched PTT film.

that is caused by the small scratch and chips on a sample surface.⁹ He claimed that it might be very difficult to obtain perfect contact between sample and ATR crystal experimentally.

In this work, the absorbance ratio was measured experimentally in order to evaluate the relationship between effective thickness ratio of two waves and quality of optical contact. Using the melt-quenched amorphous PTT film and KRS-5 double-edged ATR crystal, the A_{TM}/A_{TE} value of the 1410 cm^{-1} band was measured as a function of clamping pressure at 45° angle of incidence, and the results are shown in Figure 7. As can be seen from the figure, the ratio increases continuously as the clamping pressure increases. As the pressure increases from 20 to 35 oz/in^2 , the ratio increases from 1.1 to 1.3, which is much lower than the ideal value of 2. Very similar results were obtained for both beam paths. This fact indicates that the absorbance ratio (A_{TM}/A_{TE}) is a function of the quality of optical contact. Furthermore, it will be very difficult to secure ideal optical contact experimentally.^{9,10}

There must be a certain experimental limitation to enhance the quality of optical contact just by increasing clamping pressure because high clamping pressure might distort the sample. The ATR crystal might be mechanically damaged if the clamping pressure is applied beyond a critical value. Gupta measured the A_{TM}/A_{TE} value with a liquid sample (hexadecane) with which surface structure causing the false radiation can be minimized.⁹ Even though the absorbance ratio measured experimentally was found out to be close to the theoretical one, he claimed that it would not be easy to maintain ideal contact even with the liquid sample.

In this work, temperature of the sample and FTIR-ATR crystal was controlled to enhance the quality of optical contact. Using a temperature-controllable two-dimensional FTIR-ATR setup explained in the Experimental Section, both absorbances (A_{TM} , A_{TE}) of the 1410 cm^{-1} band were measured at two different polarization directions, and the ratios are plotted in Figure 8 as a function of temperature for three samples drawn to three different draw ratios. Measurement was repeated for both beam paths and during the cooling process also for selected samples. Since the 1410 cm^{-1} band, as a reference band for uniaxially stretched PTT, was confirmed not to be influenced by the structural parameters

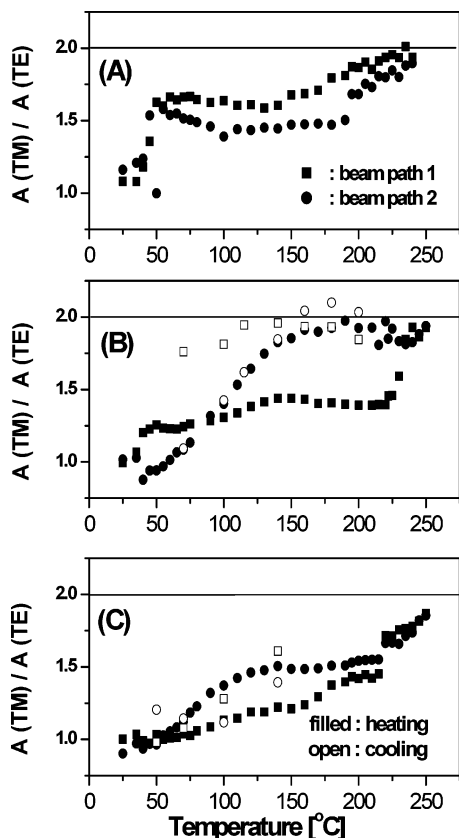


Figure 8. Absorbance ratio of TE and TM waves for the 1410 cm^{-1} band as a function of temperature: (A) melt-quenched amorphous PTT film; (B) uniaxially drawn PTT film (DR = 2); (C) uniaxially drawn PTT film (DR = 3).

such as orientation and conformation changes already, its absorbance change should be directly related to variation of the quality of optical contact between sample and ATR crystal. At room temperature, absorbance ratio of the isotropic sample was much lower than that of theoretical one (Figure 8A), which is consistent with the data in Figure 7. As the temperature increases above room temperature, the ratio increases abruptly at about 45 °C. Upon transition from glassy to rubbery state ($T_g = 45$ °C), the optical contact was suddenly improved. However, its magnitude is still smaller than the theoretical one. Its ratio shows small change up to about 150 °C (beam path 1) or 190 °C (beam path 2), and upon further increase of temperature, it starts to increase again with much higher rate. According to DSC results (data not shown), the melting endotherm of cold crystallized isotropic sample spans from about 190 to 238 °C, which approximately corresponds to the fast increase of absorbance ratio in Figure 8A. It is interesting to note that the experimental absorbance ratio of molten PTT (at $T = 240$ °C) is very close to the theoretical one. Also, it should be noted that the ratio is always smaller than the theoretical one unless the sample is in a completely molten state. Furthermore, there is a significant difference between data along the beam path 1 and the corresponding data along the beam path 2.

The absorbance ratios obtained with PTT samples uniaxially drawn-to-draw ratio (DR) of 2 and 3 are shown in Figure 8, B and C, respectively, as a function of temperature. For these samples, measurements made during cooling period are also included. Since the heated sample was cooled by a natural cooling process, data

points during cooling process are not as extensive as the ones during heating process. For both samples, the ratio at room temperature are again well below 2. Upon heating just above T_g , the sudden increase of the ratio is not as significant as the corresponding one of the isotropic sample. Even though the sample of DR = 2 showed a small abrupt increase of the ratio upon glass transition only along the beam path 1, discontinuous changes at T_g for other three cases are insignificant. To understand this results, it might be useful to recall the DSC results again. Whereas the heat capacity of the isotropic sample increased abruptly during glass transition, that of the drawn sample showed minimal discontinuous changes. With the sample drawn to DR = 4, heat capacity change during glass transition could not be clearly confirmed from its DSC thermogram. As temperature increases further above T_g , the ratio increases again with unpredictable fashions. However, it reaches close to the theoretical one when the temperature is above the melting temperature of PTT.

We found out that the contact becomes very close to an ideal one if sample turns into a completely molten state. It will be interesting to check the quality of optical contact upon cooling the completely molten sample. In general, absorbance ratio dropped below the theoretical value when temperature was lowered well below the recrystallization temperature. This result confirms again that ideal optical contact might be secured only with the completely molten sample. There are few data points that are slightly higher than the theoretical value in Figure 8B. We do not understand its origin at this moment. It might be just due to the experimental uncertainty. On the basis of the results in Figure 8, we could conclude that the quality of optical contact is far from ideal when the sample is in a solid state. It would be, therefore, almost impossible to have the effective thickness ratio of TE and TM waves close to a theoretical value during temperature scan over wide range. Furthermore, the effective thickness ratio value experimentally obtained is sensitively affected by the thermodynamic state of polymer.

Method To Eliminate the Effective Thickness Difference between TM and TE Waves. When calculating attenuation indices (k_x , k_y , k_z) of the isotropic sample with the eq 1 for a 45° angle of incidence, the experimental absorbance of the TM wave (A_{TM}) has to be twice the corresponding absorbance of the TE wave (A_{TE}) to come up with three attenuation indices (k_x , k_y , k_z) of identical magnitude. And it was mentioned in the previous section that absorbance ratio experimentally obtained is, in general, far from the theoretical value. Furthermore, in the first section of Results and Discussion, we explained the necessity of normalization process with a reference band even when using the double-edged parallelogram ATR crystal with which the remounting of sample to the ATR crystal is not necessary during measurement of a set of four spectra.

If we normalize any absorbance of a selected band with that of a reference band, the absorbance ratio of a normalized TM band to a corresponding TE band will become unity, i.e., $(A_{TM}/A_{TM(\text{reference})})/(A_{TE}/A_{TE(\text{reference})}) = 1$, provided that the sample is in an isotropic state and $\theta = 45^\circ$. Therefore, by multiplying the normalized absorbance of TM wave by 2, the normalized TM absorbance will become the theoretically expected value, which is twice the normalized TE absorbance. For any other angle of incidence, the normalized absorbance of

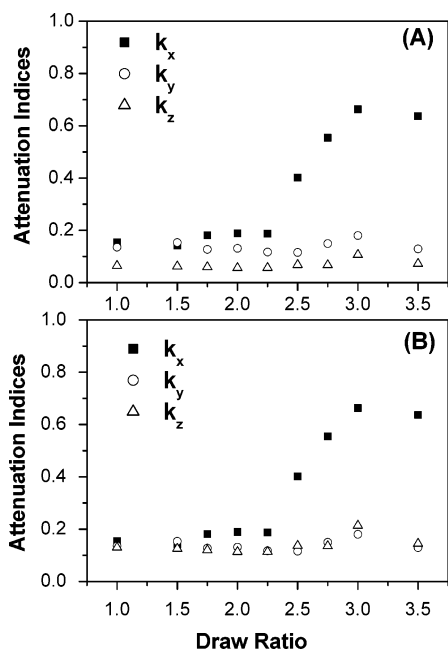


Figure 9. Comparison of results from two ATR analysis methods. Both show the changes of three attenuation indices of 1358 cm^{-1} band as a function of draw ratio for uniaxially drawn PTT films, which were calculated using the reference band (1410 cm^{-1}) without (A) or with (B) the recompensation step.

TM wave should be multiplied by $d_{e,\text{TM}}/d_{e,\text{TE}}$, the theoretical effective thickness ratio. All calculation processes discussed so far for the quantitative analysis of three-dimensional orientation analysis of PTT with FTIR-ATR spectroscopy can be summarized with the eq 4, where all symbols except P are defined already in eq 2.

$$\begin{aligned}
 A_{\text{TE,MD}}/A_{\text{TE,MD(reference)}} &= \alpha k_x \\
 P\{A_{\text{TM,MD}}/A_{\text{TM,MD(reference)}}\} &= \beta k_y + \gamma k_z \\
 A_{\text{TE,TD}}/A_{\text{TE,TD(reference)}} &= \alpha k_y \\
 P\{A_{\text{TM,TD}}/A_{\text{TM,TD(reference)}}\} &= \beta k_x + \gamma k_z \\
 P = d_{e,\text{TM}}/d_{e,\text{TE}} &= \frac{2 \sin^2 \theta - n^2}{(1 + n^2) \sin^2 \theta - n^2} \quad (4)
 \end{aligned}$$

With eq 4, the problem related to optical contact change upon rotation of sample and ATR crystal is removed by normalizing with a reference band (normalization step). The effective thickness difference, which was eliminated by the normalization process, can be brought out again by multiplying the normalized TM absorbance with the theoretical effective thickness ratio (P) (recompensation step).

In Figure 9, three attenuation indices (k_x , k_y , k_z) of the 1358 cm^{-1} band (CH_2 wagging of crystalline phase) calculated without (A) and with (B) "recompensation step" are plotted as a function of draw ratio for uniaxially stretched PTT. Since the attenuation indices in Figure 9 have been calculated using the normalized absorbance, the absolute numbers in Figure 9 are attenuation indices divided by a constant, which is the absorbance of a reference band. However, the relative magnitude between three indices should be maintained throughout the calculation process. For both data, all absorbance was normalized with that of the reference band at 1410 cm^{-1} . Both data show qualitatively a

similar dependency on the draw ratio. In Figure 9A, the attenuation indices along the transverse direction (k_y) are always higher than the corresponding ones along the normal direction (k_z). However, in Figure 9B, both indices (k_y , k_z) show an almost identical value, which is a more reasonable result for a uniaxially stretched sample showing transverse symmetry. All three attenuation indices of isotropic state ($\text{DR} = 1$) show a very similar value only if the recompensation step (Figure 9B) is applied, whereas there is a some discrepancy for data obtained without recompensation step (Figure 9A). In a few studies on three-dimensional orientation along MD, TD, ND directions of various polymers using FTIR-ATR spectroscopy, the attenuation index along ND direction has been reported to be noticeably lower than other indices even for the isotropic state.^{12,13} Those results appear to be related to the negligence of recompensation step in eq 4.

As the draw ratio increases, the attenuation index along the x direction shows a slow initial increase, followed by a sudden increase from $\text{DR} = 2.25$ to $\text{DR} = 3.0$. A sudden increase was related to a strain-induced crystallization occurring at that draw ratio range. More detailed discussion on the three-dimensional orientation and structural change of PTT upon uniaxial deformation has been already reported.¹⁹

In this work, the quantitative analysis method to obtain three-dimensional orientation information using FTIR-ATR has been explained with a polymer sample containing a reference band such as PET and PTT. An identical process can be applied for any polymer system containing a reference band. If there is no reference band, the method suggested in this work cannot be directly applied to get three-dimensional orientation information. In a paper which will be published later, we will suggest/discuss a new method to get the three-dimensional orientation information with FTIR-ATR spectroscopy for polymer systems not containing a reference band.

Conclusions

Two main experimental problems have been discussed to obtain quantitative three-dimensional orientation information on uniaxially stretched PTT sample using a polarized FTIR-ATR spectroscopy. One was the optical contact change occurring upon rotation of a sample and ATR crystal. The other was effective thickness difference between TM and TE waves. Normalizing all absorbance with that of a reference band successfully eliminated the first experimental difficulty. It was confirmed that for uniaxially stretched PTT absorbance of the band at 1410 cm^{-1} was not affected by the orientation, conformation, and crystallinity. Thus, it was successfully used as a reference band for three-dimensional orientation analysis of PTT.

When obtaining polarized ATR spectra, there was always a difference between two absorbances (A_{TM} , A_{TE}) due to the inherent difference in two effective thickness values ($d_{e,\text{TM}}$, $d_{e,\text{TE}}$). Furthermore, the ratio of two absorbances changed as the quality of optical contact between ATR crystal and sample varied. To estimate the dependency of absorbance ratio on the optical contact, the absorbance ratio was experimentally measured at various optical contact conditions that could be carried out by changing temperature of sample and ATR crystal. On the basis of this result, it could be concluded that it is almost impossible to maintain a

perfect contact between a sample in solid state and ATR crystal. For the sample studied in this work, the effective thickness ratio ($d_{e,TM}/d_{e,TE}$) approached the theoretical value as the temperature reached well above the melting temperature of PTT.

The normalization process with an internal reference band removes inevitably the difference in the effective thickness of TM and TE waves. To compensate this problem, the normalized absorbance of TM wave was again multiplied with the theoretical effective thickness ratio ($d_{e,TM}/d_{e,TE}$). With this method, quantitative three-dimensional orientation information on uniaxially stretched PTT could be successfully obtained.

Acknowledgment. This work was supported by Korea Research Foundation Grant KRF-2002-041-D00161.

References and Notes

- (1) Flournoy, P. A.; Schaffers, W. J. *Spectrochim. Acta* **1966**, *22*, 5–13.
- (2) Flournoy, P. A. *Spectrochim. Acta* **1966**, *22*, 15–20.
- (3) Harrick, N. J. *Internal Reflection Spectroscopy*, 3rd ed.; Harrick Scientific Corp., Ossing, NY, 1987.
- (4) Sung, C. S. P. *Macromolecules* **1981**, *14*, 591–594.
- (5) Hobbs, J. P.; Sung, C. S. P.; Krishnan, K.; Hill, S. *Macromolecules* **1983**, *16*, 193–199.
- (6) Sung, C. S. P.; Hobbs, J. P. *Chem. Eng. Commun.* **1984**, *30*, 229–250.
- (7) Yuan, P.; Sung, C. S. P. *Macromolecules* **1991**, *24*, 6095–6103.
- (8) Mirabella, F. M. *Appl. Spectrosc.* **1988**, *42*, 1258–1265.
- (9) Gupta, M. K.; Carlsson, D. J.; Wiles, D. M. *J. Polym. Sci., Polym. Phys. Ed.* **1984**, *22*, 1011–1027.
- (10) Kaito, A.; Nakayama, K. *Macromolecules* **1992**, *25*, 4882–4887.
- (11) Walls, D. J. *Appl. Spectrosc.* **1991**, *45*, 1193–1198.
- (12) Walls, D. J.; Coburn, J. C. *J. Polym. Sci., Polym. Phys. Ed.* **1992**, *30*, 887–897.
- (13) Lofgren, E. A.; Jabarin, S. A. *J. Appl. Polym. Sci.* **1994**, *51*, 1251–1267.
- (14) Lee, H. S.; Ko, J. H.; Song, K. S.; Choi, K. H. *J. Polym. Sci., Polym. Phys. Ed.* **1997**, *35*, 1821–1832.
- (15) Everall, N. J.; Bibby, A. *Appl. Spectrosc.* **1997**, *51*, 1083–1091.
- (16) Everall, N.; Mackerron, D.; Winter, D. *Polymer* **2002**, *43*, 4217–4223.
- (17) Bensaad, S.; Jasse, B.; Noel, C. *Polymer* **1993**, *34*, 1602–1605.
- (18) Lee, H. S.; Ko, J. H.; Song, K. S.; Choi, K. H. *J. Polym. Sci., Polym. Phys. Ed.* **1997**, *35*, 1821–1832.
- (19) Lee, H. S.; Park, S. C.; Kim, Y. H. *Macromolecules* **2000**, *33*, 7994–8001.
- (20) Park, S. C.; Liang, Y. R.; Lee, H. S. Unpublished work.
- (21) Schmidt, P. G. *J. Polym. Sci., Part A* **1963**, *1*, 1271–1292.
- (22) Fina, L. J.; Koenig, J. L. *J. Polym. Sci., Part B: Polym. Phys.* **1986**, *24*, 2509–2524.
- (23) Fina, L. J.; Koenig, J. L. *J. Polym. Sci., Part B: Polym. Phys.* **1986**, *24*, 2525–2539.
- (24) Garton, A.; Carlsson, D. J.; Wiles, D. M. *Appl. Spectrosc.* **1981**, *35*, 432–435.
- (25) Ho, R. M.; Ke, K. Z.; Chen, M. *Macromolecules* **2000**, *33*, 7529–7537.
- (26) Grebowicz, J. S.; Brown, H.; Chuah, H.; Olvera, J. M.; Wasiak, A.; Sajkiewicz, P.; Ziabicki, A. *Polymer* **2001**, *42*, 7153–7160.
- (27) Shin, D. Y.; Kim, K. J.; Yoon, K. J. *J. Korean Fiber Soc.* **1998**, *35*, 731–738.
- (28) Jang, S. S.; Jo, W. H. *Fibers Polym.* **2000**, *1*, 18–24.
- (29) Chuah, H. H. *Macromolecules* **2001**, *34*, 6985–6993.

MA0353033